THE ASTROPHYSICAL JOURNAL, 427:184–201, 1994 May 20

MODAL APPROACH TO THE MORPHOLOGY OF SPIRAL GALAXIES. III. APPLICATION TO THE GALAXY M81

S. A. LOWE,[1] W. W. ROBERTS,[2] J. YANG,[3] G. BERTIN,[4] AND C. C. LIN[5]
Received 1992 December 3; accepted 1993 November 15

ABSTRACT

The modal approach to the morphology of spiral galaxies is applied to the galaxy NGC 3031 (M81) to demonstrate how the shape of the spiral pattern, specifically that obtained by Elmegreen et al. for the distribution of the stellar objects, may be used to help with the determination of the axisymmetric basic state of a galaxy with a reasonably regular spiral structure. The parameters of the basic state are narrowly constrained when all available observational data are taken into consideration, including both the mass distribution and the two components of velocity dispersion in the stellar disk. The ratio of the two components of velocity dispersion is found to be similar to that observed in the solar vicinity—a result that supports the reasonableness of the model. The mass distribution and the mass-to-light ratio obtained agree with that given by Kent from analysis of rotation curves. When compared with the work of Visser, it appears that he might have tended to use a heavier disk to support the gravitational field without including a sufficient amount of spherical components. The success of the present modeling process also supports the view that, to a first approximation, the spiral structure in many galaxies, essentially isolated at the present time, is a long-lasting, but in general slowly evolving, largely intrinsic characteristic of a galaxy. The possible influence of the companion NGC 3077 is discussed: the global spiral structure is approximately an intrinsic mode, but its exact nature is likely to be related to an earlier passage of this small companion.

Subject headings: galaxies: individual (M81) — galaxies: kinematics and dynamics — galaxies: spiral — galaxies: structure

1. INTRODUCTION

In two previous papers (Bertin et al. 1989a, b hereafter Papers I and II), the modal approach to the global spiral structure of galaxies has been described in considerable detail. Further studies of the relevant themes within this general framework have also been published (Bertin 1990b; Lin & Lowe 1990; Bertin 1991). In these papers emphasis has been placed on the roles played by the gaseous component in the excitation and the maintenance of stable (but perhaps slowly evolving) global patterns, and on the possible importance of the existence of more than one normal mode for a given basic state. In order to test these concepts through comparison of theoretical predictions with observational data, it is desirable to choose simple cases in which a single mode *appears* to be dominating and for which fairly extensive analyses of the observational data are already available. The galaxy M81 presents itself as the natural first choice (see, e.g., Visser 1977, 1980; Kaufman et al. 1989; Kaufman, Elmegreen, & Bash 1989; Elmegreen 1990; Kent 1987a, b).

One word of caution deserves to be mentioned here: the galaxy M81 is by no means entirely isolated. The most obvious of its neighbors are M82 and NGC 3077. With the latter, there is also observed an apparent trail of H I distribution which suggests that it was even closer to M81 at some time in the past. However, it should be kept in mind that the influence of nearby companions is naturally included in the modal approach. Indeed, if the original system had only decaying modes, such a companion might even act to excite the modes, analogous to the ringing of church bells or the playing of other musical instruments. In such cases, the effect of several galaxies might be present (e.g., both M82 and NGC 3077 in the present case). Nevertheless, in many cases, the modal shape may still be well approximated by a resultant of a small number of eigenmodes with one dominating. On the other hand, global structures are observed for many field galaxies. It is therefore plausible that the internal nonlinear mechanisms in a two-component system of gas and stars would, in many instances, be able to provide a mechanism for self-excitation and maintenance of the modes. Such mechanisms have been discussed in § III of Paper I (see especially § IIIb for the discussion of the process of self-regulation in the gaseous component). It is shown there how the usual processes of wave propagation, with feedback and overreflection, can maintain a standing wave pattern, how the more subtle mechanisms of turbulent dissipation and shock formation in the gaseous component can influence the energy transfer between the basic state and the density waves, and how the process of self-regulation between gravitational instability and damping process in the gaseous component all play crucial roles in this process of self-excitation and nonlinear equilibration. In such cases, where the global structure can be self-generated, the passage of a relatively minor satellite would only serve to modify the existing modal structure (see also § 7.2).

It is with such a scenario in mind that the present study was carried out.[6] We assume that the existing spiral structure in M81 is approximately rotating as a rigid body, maintained by the nonlinear behavior of both the stellar and the gaseous

[1] Massachusetts Institute of Technology, Cambridge, MA 02139. Now at Dragon Systems, 320 Nevada Street, Newton, MA 02160.
[2] University of Virginia, Charlottesville, VA 22903.
[3] Massachusetts Institute of Technology, Cambridge, MA 02139.
[4] Scuola Normale Superiore, Piazza del Cavalieri 7, I-56126 Pisa, Italy.
[5] Massachusetts Institute of Technology, Cambridge, MA 02139. Also Florida State University, Tallahassee, FL.

[6] A brief account of this study may be found in a report by J. N. Hewitt (1991).

components. The behavior of the latter component is strongly nonlinear, but that of the former may be well described in the linear approximation. The *finite* thickness of the stellar disk is crucial here (see § 2.2). We attempt to make maximal contact with observational data, including the size and shape of the spiral pattern and its amplitude distribution. This last item is especially of interest, because better observational data are becoming available in the infrared (see, e.g., Block & Wainscoat 1991) and also in the ultraviolet (see papers published in the 1992 August issue of *Astrophysical Letters*). As it has been pointed out in several earlier publications (see, e.g., Bertin et al. 1977), amplitude modulation is expected along spiral arms in a spiral mode because of *interference* of (at least) two oppositely propagating waves, in contrast to the amplitude distribution in a single trailing density wave. Indeed, in Visser's analysis, even though he appeared to be using a single trailing wave as a first approximation, his amplitude distribution was adopted from *observational* data which would not have been predicted from the dynamical behavior for a single propagating wave packet.

The use of *observed* amplitude variation to identify the modal nature of spiral structure in galaxies was first made by Elmegreen, Elmegreen, & Seiden (1989). They placed emphasis on gas response to spiral wave resonances which may be strong enough to give observable effects, and derived pattern speeds therefrom (see Elmegreen 1990; Elmegreen, Elmegreen, & Montenegro 1993; and Elmegreen 1991, 1992). In the case of M81, they arrived at a pattern speed of 26 km s^{-1} kpc^{-1}, with a corotation circle at 8.4 kpc (a value considerably smaller than Visser's), by placing the 4:1 resonance at the observed amplitude minimum. This perception depends on the nonlinear behavior at that location. In contrast to this line of reasoning, we are making our analysis entirely within the scope of the *linear* theory, with the minimum of amplitude in the nature of an interference phenomenon shown in Figure 8 of Paper I. It is intriguing that the pattern speeds obtained by our method ($\approx$24 km s^{-1} kpc^{-1}) are not much different from their value, even though the bases of analysis are apparently quite different. This is a very interesting dynamical problem yet to be clarified (see further discussions in § 3).

With this amplitude distribution as a principal new theme, we shall make another attempt to determine a model for M81 with maximal agreement with available observational data and with the analyses of other investigators. The broad outline of the method of analysis will be described in §§ 2 and 3 (see especially §§ 2.2 and 3.2 for features beyond Paper I). The results for the model obtained are described in the subsequent sections, together with comparison with other observational data, including those of the amplitude distribution of the density wave, and the distribution of the gaseous component and its flow field. We shall find that the *shape* and the *amplitude* distribution of the spiral structure are the two functions that determine the distribution of the two components of velocity dispersion of the stars.

Certain assumptions have been adopted here, in common with other earlier studies of other authors, in order to make the analysis possible. For example, the optical observations suggested an exponential mass distribution on the basis of the *assumption* that the mass-to-light ratio M/L is uniform over the disk. Alternative models may be obtained based on dynamical considerations (Bertin 1991) without using this assumption (see § 7). This will be left for future investigations. In this paper we present a range of possible basic models for M81 which would support a spiral *mode* that appears to be, in a first approximation, to be consistent with a number of observational features. For one of them we give very detailed analyses. For another, we presented enough details to show that the same general conclusions are supported.

The new model determined will be found to be significantly different from Visser's model, which has little spherical component and a significantly more massive disk. The pattern speed determined from such a model is naturally considerably lower (18 km s^{-1} kpc^{-1}) than that determined in this paper (24 km s^{-1} kpc^{-1}) with corresponding shifts in the location of the corotation circle and major resonances. But it should be made clear that an encouraging development for our line of studies is the increasing amount of data through infrared observations in a number of galaxies. In contrast, for M81, the data in the red and the near-infrared are still of limited accuracy. We shall see how they are combined with other data to carry through our calculations (see § 3).

It should be made clear that the principal objectives of this paper go beyond a reasonably accurate determination of a model for M81 or a (narrow) range of possible models. Besides using this special example for demonstrating the general validity of the modal approach, we primarily have in mind the following two more specific objectives. First, we wish to present a method of analysis that may be applied to any galaxy when appropriate observational data become available. Second, we wish to show, with M81 as an example, that the modal approach does *not* require *unreasonable* physical basic states even when several rather detailed observational constraints are placed on the model. The modal approach also receives support from recent calculations using N-particle simulation for two component systems (Thomasson et al. 1990; Elmegreen & Thomasson 1993). By using a model with the rotation curve of M81 and with a galactic disk of the same overall characteristics (see § 2.2 for further discussion of this point), these authors obtained modal patterns which show general characteristics similar to those observed. Thus, even though most of the detailed comparison with observational data is only made in the present paper, the general theme of the modal formation is supported by both approaches, in contrast to the scenario that the spiral structure is a transient structure produced by the passage of NGC 3077 (see § 7.2 for further discussion).

2. METHOD OF ANALYSIS: OBSERVATIONAL CONSTRAINTS

In order to give a specific demonstration of the viability of the modal approach, we set as our primary objective the determination of a model for the basic state of M81 that would support a mode compatible with the spiral pattern observed, and with other observational data, according to the dynamics of a two-component system of stars and gas. In other words, we wish to have a composite star-gas model within the major observational constraints in the spirit of the modal approach. For this purpose, it is natural to follow a procedure of *successive approximations* as we gradually increase the scope of the constraints from existing data and make more predictions for comparison with future observations.

This procedure consists of three steps, the construction of

1. a model with a single fluid component distributed in a disk of infinitesimal thickness,
2. a two-component model with stars and gas in which the small but *finite* thickness of the stellar disk is considered, and
3. a model in which the nuclear bulge and the halo mass are included.

The significance of the third step will be explained below in the relevant sections. In both steps 1 and 2, the focus is on the galactic disk that would support the observed spiral pattern. Once the rotation curve is given, these steps are independent of step 3.

2.1. *One-Component Systems*

Successful modeling of the spiral pattern depends on the reproduction of two *observed* distribution functions: (1) the pitch angle of the spiral arms, and (2) the *amplitude distribution* along the spiral arm. In a spiral *mode*, which is composed of incoming and outgoing waves, the interference of these waves leads to amplitude *modulation*. This feature is very important because it distinguishes between a propagating wave packet and a wave mode. We thus need two functions in the basic state at our disposal in order to be successful. These are (1) the velocity dispersion in the *radial* direction (or some appropriate Q-parameter), and (2) the velocity dispersion in the *vertical* direction (or the thickness distribution of the galactic disk). Thus the problem is well defined.

We start with the type of model described in Paper I with a single fluid component distributed in a disk of infinitesimal thickness, that is, a one-component disk system in two-dimensional distribution, or briefly, a (1C/2D) model. A computational program has been developed for this purpose (see Paper I) when three distribution functions are specified through a limited number of parameters. Observational information is taken into account in the choice of such functions. For example, the exponential disk was adopted for the surface density (plus a small modification from gaseous mass). There are only two parameters: the magnitude scale and the length scale. The rotation curve was taken in the form of a simple interpolation formula which agrees with the essentials of the observational data. The distribution of velocity dispersion is chosen through the choice of Bertin-Romeo's Q-parameter $Q_{\rm eq}$ in the form of a Gaussian distribution so that the inner disk is inhospitable to wave propagation. Here, we also impose one important constraint from physical and dynamical considerations; that is, we argue that the outer gas-rich galactic disk must be close to a condition of *marginal* gravitational instability with respect to axisymmetric disturbances ($Q_{\rm eq} \approx 1$) because of the process of self-regulation through gravitational action, turbulent dissipation, etc. (see Bertin and Romeo 1988; Paper I; Bertin 1991; see also Romeo 1992).

With this particular class of models at hand, we can make a survey of modal shapes as the parameters are varied. This has been carried out extensively in Paper I for the modes with the highest pattern speed in each model. Data including other modes were available but given limited publication (see, e.g., Lin & Lowe 1990). From our experience, it is clear that the characteristics of the modes obtained are more sensitive to changes in some of the parameters than others. For example, a relatively small change in the parameter Q_{OD} (Q in the outer disk) could lead to a considerable change of the growth rate, in the amplitude distribution, or even in the modal shape; a substantial increase in Q_{OD} could make all the models stable. Such behavior must be understood from the physical point of view (as mentioned above) and mastered from the numerical point of view in order to finalize the determination of the model. More about these points later (see also sections on final results).

Another point to be emphasized in the studies of modal approach is the distinction between the *early* stages of the solution of an initial value problem and the asymptotic behavior in *late* stages. Modal characteristics show up in the late stages (see Paper I, last paragraph in Appendix C). Fortunately, in the context of global modes, we are dealing with genuine wave propagation at a relatively high speed, and with a dispersive and dissipative medium; hence the late stage will be reached in a *relatively short* period of time.

Further discussion of the detailed procedures will be given below in § 3.

2.2. *Two-Component Systems*

For comparison with observational data, there are obvious limitations in the use of the simple one-component model just described. Visser (1977, 1980) constructed models with finite thickness for the galactic disk for a two-component system, on the basis of the spiral structure. Kent (1987a, b) studied mass models that include a luminous nuclear bulge without reference to the spiral structure. Thus, the *physical* model should be a two-component model in three-dimensional distribution, or (2C/3D) models in constrast to (1C/2D) models used for studying the *dynamics* for the formation of models. Indeed, the dynamical *equilibration* of the calculated unstable modes into a long-lasting stable state depend very much on the gaseous component.

Since the computation program has originally been developed for the (1C/2D) models, we must be able to relate a (2C/3D) model formulated to a suitable (1C/2D) model. This may be accomplished, for example, by using the finite thickness *reduction factor* calculated by Shu (1968, 1971) and by Vanderhoort (1970) and adopted by Yue (1982) for application to modal calculations. We adopt a two-component model with finite thickness only for the stellar disk, since we found that the small thickness of the gaseous disk is insignificant. The reduction factor depends on the dimensionless parameter kz_*, where k is the local wave number of the observed pattern, and z_* is the local thickness of the galactic disk. Fortunately, for the inverse problem at hand, k is known. On the basis of suggestions of several observers z_* is taken to be constant for simplicity in most of the calculations. It replaces the scale length in the reduction factor in Paper I as a parameter at our disposal, and the reasonableness of its choice can be checked with observable quantities. (See below for discussions of the ratio of c_{*z}/c_{*r}, the dispersion velocities in the perpendicular and radial directions in the disk.)

There are two risks in adopting models of zero thickness: (1) the problem of "overheating" in N-particle simulation, and (2) the exaggeration of the *nonlinear* effect of the gaseous component. The former is well known among experts in N-particle simulation, and several ingenious methods have been adopted to address, it including the softening of interaction among the particles, replacing the "hot particles" with "cool" or "cold particles" and the introduction of a "mathematical" coefficient of dynamical friction (Toomre & Kalnajs 1991). These are issues which would arise in the present context only when we attempt to compare our results with those obtained from N-particle simulation (e.g., Elmegreen et al. 1993). Our attention is directed to the second point, which was first brought up by Lubow, Balbus, & Cowie (1986) and examined in greater detail by Lubow (1988). These authors might have overestimated the nonlinear effects of the gaseous component.

To see the issues involved, consider a reasonably realistic model with a stellar disk of finite thickness and a gaseous disk of much smaller thickness. The linear theory of density waves

for a galactic disk of finite thickness had been developed by Shu (1968, 1971) in which corresponding or "equivalent" models of zero thickness has been developed. (The theory for the stellar disk alone had also been carried out in a different and possibly better approximation by Vandervoort 1970; but the results are essentially in agreement.)

In the examination of nonlinear behavior of the gaseous component, Lubow et al. did not go through this process. Had they attempted to do so, they would have found that the perturbations in the gaseous disk on the smaller scales ("higher harmonics" to the fundamental) would have a much reduced impact on the behavior of the stellar system (except possibly near the galactic shock), which is thick and therefore much more stable because of its significantly three-dimensional nature in the context of the perturbations of smaller horizontal scales in the gaseous disk. The relationship between the gaseous and the stellar components is much less symmetrical than in the linear theory. One important conclusion is that the nonlinear behavior of the gaseous component would not have the disruptive behavior that might be expected had both components been placed in a disk of zero thickness (see infrared data of Bloch & Wainscoat cited above). The stability of the stellar disk is not only due to its large velocity dispersion in the disk, but also due to that perpendicular to it. This is another reason why it is important to construct models of the type described in this paper.

2.3. *Models Including Spherical Components*

In Visser's study of M81, the rotation curve is supported essentially by the mass in the disk. This leads to a *higher* disk mass than that obtained by other more careful studies of mass models (see, e.g., Kent 1987a, b). The higher disk mass leads naturally to a *lower* value of the pattern speed if the same pitch angles are to be obtained. Indeed, as we shall see, Visser's value, $\Omega_p \cong 18$ km s^{-1} kpc^{-1}, is quite a bit lower than our value of approximately 24 km s^{-1} kpc^{-1}. The inner limit of the spiral pattern is observed to be close to 4 kpc, and Visser's value would imply that this is approximately located at inner Lindblad resonance. This is unlikely to be the case, since a prominent ring would be observed like that in NGC 5364 at resonance, or the waves are absorbed. It is rather more likely that the waves are mainly refracted into leading form at $r \cong 4$ kpc. Indeed, our modal calculations show a rapid decline of wave amplitude from $r = 4$ kpc inward consistent with the concept that this is where the inner turning point r_{ce} is located.

The above discussions show the need for the construction of a detailed mass model including the spherical component. Such a model for M81 has been given by Kent (1987a, b), for a disk of zero thickness. We made *independent* analysis with disk mass already determined from modal analysis. We found, however, very satisfactory agreement between our model and his model. This model construction leads us to a value for the mass-to-light ratio $M/L \approx 4$ which is considered to be typical for the disks of SB galaxies of the general type of M81 (see Kent 1987a, b).

2.4. *Components on Other Observational Constraints*

After our model is tentatively established, we attempt to make a number of specific inferences from our model; for example, predictions on the observed flow field and the ratio c_{z*}/c_{r*}, in order to make sure that our model is generally "reasonable." We do not go into details here, but leave further analyses to future studies, since these would depend on other assumptions; for instance, the physical model for the interstellar medium. Our primary objective in this paper is to show that the use of the modal approach, together with the observational data for the distribution of the red and infrared components, can lead to a reasonable model for M81 that is compatible with a number of other observational constraints. In fact, the determination of the angular velocity of the wave pattern from purely *kinematic* considerations of the conservation of H I mass leads to approximately the same numerical value of Ω_p (Westpfahl 1993) as we found here for our mode, provided that it is assumed that the spiral structure in M81 is approximately rotating as a rigid body with little change in shape. If this assumption were rejected, then the pure kinematic analysis of type used by Westpfahl has to be modified to include radial propagation of spiral waves (see Toomre 1981, Fig. 8) since radial gradients of density distribution are much higher than circular gradients (by a factor of about 5 in the present case) and the group velocity for radial propagation is considerable.

3. MODELS FOR THE GALACTIC DISK

We shall now address the procedure to construct galactic models for the basic state that would support spiral modes with the observed modal shape and density distributions. We would further like to check the distribution and the flow field of the interstellar medium observed against the theoretically computed results from our model. As we shall see, there are a number of observational data to be fulfilled and a number of parameters to be varied in our model. It is therefore not an easy task to carry out the calculations to find a satisfactory model To make the procedure tractable, we shall divide it into two steps.

The first step, to be described in § 3.1, is to adopt the "E-models" described in Paper I. These are one-component *dynamical* models with an exponential mass distribution and a galactic disk of zero thickness. These are referred to as (1zt) models or (1C/2D) models. The procedure for modal calculation is given in Paper I.

In the second step, to be described in § 3.2, we consider *physical models* with separate specifications of the characteristic of the stellar and the gaseous components, with a finite thickness assigned to the stellar component. These are referred to as (2ft) models or (2C/2D) models. They are the final answers to be sought and compared with similar models given by Visser and with observational data available. These models all contain specifications of the velocity dispersion of stellar velocities both along the radial direction and perpendicular to the galactic disk.

It would have been most welcome if the parameters of the physical models can be inferred from the dynamical models. Unfortunately, this is not the case. For one thing, the reduction factor used in § 3.2 is different from the quartic used in Paper I, although they are numerically quite close. One can only use the dynamical model as a first approximation and as a guide. (Technically, the "input parameters" are quite different in the two calculations.)

In the construction of models, on the basis of observational data, it is natural that there are "error bars"; that is, we should examine a range of models to get a feeling of how accurate our results are. If the possible range is quite wide, we would be disappointed with the whole approach. Fortunately, the flexibility in the determination of the model is quite limited.

Two models have been examined in substantial detail. They are quite similar in general characteristics, and both give support to the essential points of our investigation described in § 1. Since the details are quite complicated, we shall describe only one of them in complete detail in this paper. The other model will be discussed, in comparison with the first model, § 3.3, to demonstrate the "error bars" in our analysis.

In all the analysis of the modal structure in this paper, the linear treatment of the gaseous component is adopted, even though its full nonlinear behavior is taken into account when its response to the resultant gravitational potential is calculated. This is based on the fact that M81 is not a gas-rich galaxy. Consequently, the gaseous component has only a limited impact on the behavior of the stars. With a large fraction of gas present, its nonlinear effect may even distort the characteristics of freely propagating density waves (see Lubow et al. 1986; Lubow 1987). But even here the finite thickness of the galactic disk would significantly reduce the nonlinear effect, since they are associated with higher harmonics of shorter wavelength. In general, a process of successive approximations is needed.

3.1. *Models with Zero Disk Thickness*

We now turn to the discussion of the 1C/2D model with distribution functions described in Paper I. For convenience of reference, we reproduce the relevant formulas as follows:

$$V(r) = V_{OD}\left[1 + \left(\frac{r_\Omega}{r}\right)^2\right]^{-1/2} S(r)\,, \tag{3.1a}$$

$$\sigma(r) = \hat{\sigma}_0(1 + \Delta)e^{-r/h} f\left(\frac{r}{r_{\rm cut}}\right), \tag{3.1b}$$

$$Q(r) = Q_{OD}\left\{1 + q\,\exp\left[-\left(\frac{r}{r_Q}\right)^2\right]\right\}, \tag{3.1c}$$

where $f(r/r_{\rm cut})$ is given by a quartic polynomial, and

$$S(r) = \left[1 + \left(\frac{r}{r_s}\right)^4\right]^{-1/4(s_{OD}-1)}. \tag{3.2}$$

The numerical values used for the three parameters are $V_{OD} = 275$ km s^{-1}, $r_\Omega = 2$ kpc, $r_s = 5.3$ kpc, and $s_{OD} = 1.34$. The mass distribution for supporting such a rotation curve will be discussed in § 4.

There are thus the following five parameters available to us for adjustment to fit observational data: Δ, Q_{OD}, q, r_Q, and $r_{\rm cut}$. We regard the exponential scale factor as well determined from observational data. The parameter Δ is obviously related to the mass-to-light ratio M/L which is not well known. Indeed, it will appear as one of the "predictions" from our analysis. We assume a uniform value for M/L over the disk. In the next section we shall see how $r_{\rm cut}$ is related to the thickness of the stellar disk.

To fit the observational data for the intensity distribution of the stellar component (Elmegreen et al. 1989) we proceed as follows. From the Fourier decomposition

$$I(r, \theta) = \sum_m a_m(r)\cos\left[m\theta + \varphi_m(r)\right], \tag{3.3}$$

we single out the second harmonic ($m = 2$), and plot $a_2(r)$ versus r. This results from the *interference pattern* of leading and trailing waves propagating in opposite directions (see Fig. 2).

As already emphasized by Bertin et al. 1977), the amplitude modulation is the principal characteristic that distinguishes between a single propagating group of waves and a mode consisting of at least two waves propagating in opposite directions. Thus, we choose the following four parameters in this interference pattern as the *targets* for comparison between theoretical predictions and observational data (see Figure 3 and further explanation of symbols):

1. $r_{\rm min}$ (or r_1),
2. $A_{\rm max}/A_{\rm min}$ (or A_1/A_2),
3. $r_{\rm max2}/r_{\rm max}$ (or r_3/r_1),
4. $A_{\rm max}/A_{\rm max2}$ (or A_1/A_3).

In this list the location of the dip in amplitude is denoted by $r_{\rm min}$. The two maxima are designated by max and max2: thus their amplitudes are, respectively, $A_{\rm max}$ and $A_{\rm max2}$, and the locations of their central points are, respectively, $r_{\rm max}$ and $r_{\rm max2}$. Alternatively, the symbols may simply carry subscripts 1, 2, and 3 in the order of first maximum, minimum, and second maximum. The first two items are clearly visible reference features in photometry, and they depend very much on the phenomenon of interference. The third item, dependent on the separations of the humps, is clearly related to the wavelength of the pattern (and hence the pitch angle). The last item refers to the general trend in the amplitude distribution of the wave pattern. This is possibly the least reliable of the four targets, since the magnitude of $A_{\rm max2}$ could depend on the behavior of the gaseous component.

The four *control* parameters (i.e., the parameters at our disposal for reaching our targets) are the first four listed earlier (Δ, Q_{OD}, q, r_Q). Only two values were chosen for the fifth parameter $r_{\rm cut}$ in our survey. Indeed, its value may be better judged from the discussion of disk thickness and other observational data (see below). To get optimal models, we have to carry out an extensive survey as the control parameters are varied. If three values were chosen for each of the four parameters, we would have a total of 81 cases; with two choices for $r_{\rm cut}$, we would be dealing with 162 cases.

Based on the results obtained for a number of cases, we are able to get a general sense to anticipate the trends for changes of the theoretical values of the target parameters as the control parameters are varied. Based on this experience, we performed a systematic survey from which we select a range of optimal models in the 1C/2D framework for further studies and comparison with other available observation data. We can then use such models as a first approximation and as a basis for constructing the 2C/3D models. Although our primary attention is on the amplitude distribution $a_2(r)$, we must impose the following criteria for reasonableness of the models: (1) the corotation circle must be well located so that the flow field would be in reasonable agreement with observational data; (2) the growth rate γ should be moderate; and (3) the pitch angle i should be close to that observed so that the observed spiral pattern may be well reproduced. The results presented in the attached tables are selected from a much more extensive survey. (In all these cases, the parameter $q = 2.6$.)

In Table 1 we exhibit a broad survey for the case of a thin galactic disk with $r_{\rm cut} = 3h_*$, $r_Q = 3.5$ kpc. (The relationship between $r_{\rm cut}$ and disk thickness will become clear in the next section.) In this table the optimal case is that with

$$Q_{OD} = 1.10 \quad \text{and} \quad \Delta = -45\%\,.$$

TABLE 1

A BROAD SURVEY OF MODES FOR THE CASE OF SMALL DISK THICKNESS ($r_{cut} = 3h_*$)

Q_{OD} \ Δ	−50%	−45%	−40%	−35%	−30%	−25%	−3%	Item
1.30.....	1.622	1.652	1.681	...	1.714	1.740	...	R_3/R_1
	1.333	1.348	1.362	...	1.367	1.380	...	R_2/R_1
	6.000	6.204	6.396	...	6.696	6.900	...	R_2
	0.795	0.750	0.723	...	0.711	0.711	...	A_3/A_1
	0.046	0.071	0.121	...	0.207	0.226	...	A_2/A_1
	20.303	20.248	20.153	...	19.732	19.403	...	Ω_p
	0.142	0.269	0.568	...	1.354	1.703	...	γ
	17.251	17.963	18.714	...	19.632	20.080	...	i(deg)
1.25.....	1.565	1.596	1.625	...	1.694	1.700	...	R_3/R_1
	1.304	1.319	1.333	...	1.367	1.360	...	R_2/R_1
	6.000	6.204	6.396	...	6.696	6.804	...	R_2
	0.833	0.783	0.770	...	0.775	0.772	...	A_3/A_1
	0.076	0.112	0.198	...	0.303	0.313	...	A_2/A_1
	21.111	21.150	21.123	...	20.799	20.502	...	Ω_p
	0.184	0.379	0.842	...	1.893	2.278	...	γ
	16.117	16.945	17.817	...	19.328	19.461	...	i(deg)
1.20.....	1.543	1.596	1.625	...	1.673	1.680	...	R_3/R_1
	1.283	1.319	1.313	...	1.347	1.340	...	R_2/R_1
	5.904	6.204	6.300	...	6.600	6.696	...	R_2
	0.883	0.836	0.834	...	0.863	0.861	...	A_3/A_1
	0.103	0.168	0.277	...	0.410	0.429	...	A_2/A_1
	21.989	22.126	22.206	...	21.912	21.637	...	Ω_p
	0.208	0.476	1.077	...	2.443	2.998	...	γ
	15.698	17.001	17.820	...	18.822	18.925	...	i(deg)
1.15.....	1.511	1.542	1.571	...	1.60	...	...	R_3/R_1
	1.255	1.292	1.286	...	1.280	...	...	R_2/R_1
	5.904	6.204	6.300	...	6.396	...	...	R_2
	0.951	0.906	0.941	...	0.976	...	...	A_3/A_1
	0.087	0.204	0.373	...	0.532	...	...	A_2/A_1
	22.978	23.267	23.386	...	23.125	...	...	Ω_p
	0.139	0.496	1.338	...	3.053	...	...	γ
	14.914	15.920	16.704	...	17.437	...	...	i(deg)
1.10.....	...	1.500	1.510	...	1.549	1.569	1.667	R_3/R_1
	...	1.260	1.235	...	1.235	1.255	1.314	R_2/R_1
	...	6.300	6.300	...	6.300	6.396	6.696	R_2
	...	1.022	1.086	...	1.110	1.098	0.993	A_3/A_1
	...	0.332	0.538	...	0.671	0.680	0.608	A_2/A_1
	...	24.708	24.842	...	24.490	24.163	22.408	Ω_p
	...	0.723	1.877	...	3.818	4.560	6.626	γ
	...	14.903	15.191	...	16.127	16.551	18.513	i(deg)
1.00.....	1.321	1.358	1.377	1.370	1.389	1.407	1.549	R_3/R_1
	1.179	1.170	1.113	1.056	1.074	1.093	1.235	R_2/R_1
	6.600	6.204	5.904	5.700	5.796	5.904	6.300	R_2
	0.929	1.189	1.369	1.446	1.422	1.377	1.209	A_3/A_1
	0.597	0.763	0.929	0.993	0.995	0.980	0.850	A_2/A_1
	27.792	27.681	27.528	27.421	27.335	27.151	25.457	Ω_p
	1.166	2.514	4.201	5.735	6.733	7.541	9.577	γ
	10.458	11.316	11.815	12.308	12.965	13.509	16.239	i(deg)

NOTE.—The growth rate γ is too high for all the cases with high Δ. The optimal choice is the case $Q_{OD} = 1.1$ and $\Delta = -45\%$, even though the ratio A_2/A_1 is already somewhat too low compared with the value 0.4 estimated from observational data. The case $Q_{OD} = 1.15$ and $\Delta = -45\%$ has an even lower value of A_2/A_1. Data are for the case with $r_{cut} = 3h_*$ and $r_Q = 3.5$ kpc.

The pitch angle is 15°, and

$$\Omega_p = 24.7, \quad \gamma = 0.723$$

(in km s^{-1} kpc^{-1}). The location of the dip $R_2 = 6.3$ kpc is quite reasonable, but the amplitude ratio $A_2/A_1 = 0.332$ is slightly too high. The ratio of the two maxima $A_3/A_1 \simeq 1$ is too high for the blue data but within range of the data for near-infrared, which is unfortunately too faint and therefore quantitatively unreliable.

More reasonable models are shown in Table 2 in which the galactic disk is thicker ($r_{cut} = 6h_*$, $r_Q = 3.5$ kpc). Here we see a range of possible models with fairly reasonable values of the principal target parameters

$$A_3/A_1 \simeq 0.7\,, \quad A_2/A_1 \simeq 0.45\,,$$

and the pitch angle i in the range 12°–15°; the location of the dip is also very close to that observed. Furthermore, all these models have moderate values of the growth rate and reasonable values for Ω_p (22.3–24.3 km s^{-1} kpc^{-1}). The control parameters Δ and Q_{OD} lie approximately in the range of (−30%, −25%) and (1.10, 1.20).

On the basis of these data, we can construct the 2C/3D models (see § 3.2). The comparison between the results for the optimal model with observational data is shown in § 6 as

TABLE 2

LIMITED SURVEY FOR THE CASE OF THICKER STELLAR DISK ($r_{cut} = 6h_*$)

Q_{inf} \ Δ	−35%	−30%	−25%	−3%	Item
1.20.....	...	1.449	1.469	...	R_3/R_1
	...	1.245	1.265	...	R_2/R_1
	...	6.096	6.204	...	R_2
	...	0.627	0.645	...	A_3/A_1
	...	0.322	0.453	...	A_2/A_1
	...	22.332	22.509	...	Ω_p
	...	0.393	2.391	...	γ
	...	14.145	15.111	...	i(deg)
1.25.....	...	1.420	1.440	...	R_3/R_1
	...	1.220	1.240	...	R_2/R_1
	...	6.096	6.204	...	R_2
	...	0.677	0.720	...	A_3/A_1
	...	0.381	0.541	...	A_2/A_1
	...	23.157	23.325	...	Ω_p
	...	0.390	0.847	...	γ
	...	13.334	14.151	...	i(deg)
1.10.....	1.358	1.377	1.385	1.327	R_2/R_1
	1.189	1.208	1.212	1.212	R_2/R_1
	6.300	6.396	6.300	6.300	R_2
	0.682	0.705	0.777	0.939	A_3/A_1
	0.136	0.453	0.629	0.930	A_2/A_1
	23.973	24.227	24.367	24.530	Ω_p
	0.087	0.458	0.972	3.885	γ
	11.106	12.125	12.789	14.865	i(deg)

NOTE.—The growth rate γ is generally reasonable. Both the cases (Q_{OD}, Δ) = (1.10, −30%) and (1.20, −25%) are acceptable models. The former gives an approximated pitch angle of 12° and the latter, 15°. The density distribution plotted for the former case appears to agree better with the data observed. Data are for the case with $r_{cut} = -6h_*$ and $r_Q = 3.5$ kpc.

Figure 3. Clearly, the shape of the curves near the maxima are not exactly the same, since the flat tops in the data are influenced by nonlinear effects not reproducible in a linear theory.

Indeed, in our theory, nonlinear effects play an important role in the equilibration of the growing mode, but we have as yet not attempted to incorporate this effect in our calculations. Nevertheless, the general agreement obtained supports two plausible conclusions: (1) the interference pattern suggests that the spiral pattern is a standing wave pattern of the modal type and (2) the basic state arrived at is a reasonable first approximation (upon which improvements will be made below).

At this point it is appropriate again to refer to Elmegreen's study of amplitude variation based on resonances. Note that this particular survey of linear modes provides the possibility of models with $\Omega_p = 26$ km s^{-1} kpc^{-1}, but unfortunately only in those cases with quite high growth rates. This gives additional incentive for the study mentioned in § 1 of the *nonlinear* behavior of the modes (especially of the gaseous response) to decide how important a role on amplitude variation is played by resonances.

The two values of Ω_p (24, 26 km s^{-1} kpc^{-1}) differ by less than 10%, which is well within the range of values for various possible theoretical models discussed in this paper. Since the construction of such models is based on the observed amplitude for mass distributions, the observational data used should preferably be those in the infrared, at about 2 μm. Until such data become available with good accuracy, further attempts to improve this agreement may not be warranted.

In the meantime, if we continue to associate the amplitude variation with the linear modes, we have also been able to get reasonable models with higher pitch angles (~15°) preferred by the radio astronomers (Visser 1977; 1982; Rots 1975). Such a model was obtained through a systematic change of the parameters (a rather elaborative process); it has a pattern speed of approximately 22 km s^{-1} kpc^{-1}.

It is perhaps reasonable to draw the following tentative conclusion. Both the linear interference of stellar waves and the nonlinear response of the gas at 4:1 resonance provide the possibility to cause a maximum to be observed in the amplitude distribution of the blue objects. The contrast in amplitude may therefore be expected to be most prominent when these two effects reinforce each other. This might be happening in M81.

In other galaxies, the two mechanisms might not yield pattern speeds in close agreement. Indeed, one might speculate that the observational data in blue and in infrared might show different minima in amplitude distribution. It would be very desirable to have such infrared data on amplitude distribution.

3.2. *Models with Finite Thickness for the Stellar Disk*

Now that a satisfactory range of dynamical models has been obtained for M81, we may turn our attention to the step of treating the effect of finite disk thickness of the stellar disk more explicitly. The thickness of the gaseous disk will still be neglected. The difference from the above will be in the reduction factor $f(r/r_{cut})$. Since the pitch angle of the spiral structure is a given observed quantity, we can make an explicit application of the theoretical results for the thickness reduction factor of Shu or Vandervoort. After the thickness correction is introduced, the equivalent Q-parameter of the disk may be determined according to the theory of Bertin & Romeo (1988). For a further treatment of the stability of thick two-component galactic disks, see Romeo (1992).

The observed luminosity distribution is well known to be exponential. A uniform mass-to-light ratio M/L is usually assumed, but its numerical value is not well determined, and is indeed to be determined from the present study as well as from other studies. We start with the formula

$$\sigma_* = \hat{\sigma}_* \exp\left(\frac{-r}{h_*}\right), \tag{3.4}$$

where h_* can be determined (with certain limits of error) from empirical data.

According to Shu (1986, 1971) and Vandervoort (1970), the active disk mass is reduced from equation (3.4) by a reduction factor which is of the form

$$T_{**} = T_{**}(|k|z_*) \tag{3.5}$$

for the stellar component, where $|k|$ is the wave number of the spiral structure and z_* is the thickness of the galactic disk. The numerical values given by the two authors are slightly different from each other, but we find it convenient and sufficiently accurate to use the formula

$$T_{**} = \exp(-|k|z_*). \tag{3.6}$$

For comparison with observational data, we find it convenient to write

$$|k|z_* = \frac{h_c}{r} \quad \text{with } h_c = m \cdot z_* \cdot \cot i,$$

where i is the pitch angle and m is the number of arms ($m = 2$

for our main purpose). Thus, the effective active surface density may be written as[7]

$$\sigma_{\rm eff} = \hat{\sigma}_* \exp\left(-\frac{r}{h_*} - \frac{h_c}{r}\right) \tag{3.7}$$

(where h_* and h_c happen to be nearly equal to each other in our particular example). The distribution $\sigma_{\rm eff}(r)$ is thus very different from the original exponential disk (see Figs. 1 and 2 in Paper I).

Of the parameters defining h_c, i is readily observable, but z_* is not; h_c is thus a parameter at our disposal. However, since there are indications that z_* is nearly constant in the outer disk and we are often dealing with logarithmic spirals, h_c may be taken to be a constant in a first approximation.

In the *bulge* region of M81, however, there is no spiral structure, and thus the formula (3.4) is not relevant. Instead, there should be a correction factor $g(r)$

$$\sigma_{\rm eff} = \sigma_* \exp\left(-\frac{r}{h_*}\right) g(r) \tag{3.8}$$

which should approach to zero very quickly as $r \to 0$; but the precise form of $g(r)$ is not known, nor is its precise form critical, since there is no wave propagation in this region. We note that the factor $\exp(-h_c/r)$ fulfills the requirement just mentioned. Thus, for simplicity, we may take equation (3.6) as an extrapolation into the bulge region for the purposes of our analysis even though its physical basis is different. Thus, we may also allow reasonable changes in the parameter h_c on the basis of qualitative physical arguments[8] the discussion in the previous paragraphs apply (see Appendix A for further details).

The above discussions allow us to start with a three-dimensional *physical* model to deduce a two-dimensional *dynamical* model by applying an appropriate reduction factor to the stellar disk. A similar discussion should be done for the gaseous disk, but the reduction factor is less important in view of the small disk thickness. All these are essentially the same as in Paper I. The final procedure for computer calculation has been written out by S. A. Lowe into the form of a program called EIGENMODE (it is available upon request).

In principle, the procedure of calculation is one of *trial and error of iteration*. However, experience and qualitative physical arguments allow us to proceed with little difficulty, and there is considerable room for refinement. For example, the thickness parameter z_* should be on the order of (0.30 ± 0.20) kpc if one compares M81 with the Milky Way system, and it need not be strictly constant. Also, the pitch angle found by following Shu's (1968, 1971) procedure of using local dispersion relationship has been found to be useful, because it is found to give results in agreement with that calculated from the modal procedure. Iterative calculations are generally needed to get desired results, but they were not found to be necessary in the present case, largely because we already start with reasonable models obtained in § 3.1 (see also Appendix B). The final results obtained and the comparison with observations may be found in § 4.

[7] We need not take the exponential formula for T_{**} to be exact in order to get a formula of this general form. We may simply introduce a parameter $h_c(r) = -r \ln T_{**}$ as the function at our disposal which is approximately equal to $h_c(r)$ defined by eq. (3.6). Indeed, one objective of the modeling process is an attempt to determine $h_c(r)$.

[8] The resultant reduction factor is finally given in the form $\bar{f}(x) = \exp\{-1/6x[1 + w\exp(-16x^2)]\}$, where w is at our disposal (with $w = 0$ corresponding to uniform disk thickness), and $x = r/6h$. In the spiral region, this form corresponds to a uniform disk thickness of 0.30 kpc, if the pitch angle is 12° in the bulge region. It is just an extrapolation formulation with a surface density approaching zero rapidly as $r \to 0$.

3.3. *Discussion*

It would be desirable to carry out a survey similar to that presented in Tables 1 and 2 but based on the parameters that appear in § 3.2. Unfortunately, this would be quite an elaborate program. Instead, we pick two reasonable models—to create a range—from Tables 1 and 2 and use them as *approximations* to get physical models on the basis of § 3.2. The two cases chosen are those in Table 2 with (Δ, Q_{OD}) respectively, equal to $(-35, 1.1)$ and $(-25, 1.2)$. The principal characteristics of the final models for these two cases are listed as follows:

1. z_*(kpc) = 0.30, $Q_{OD} = 1.1, \Delta = 35\%, i = 12°, \Omega_p = 24.2$;
2. z_*(kpc) = 0.15, $Q_{OD} = 1.2, \Delta = 25\%, i = 15°, \Omega_p = 22.2$.

Both cases have been pursued in some detail to assure us that they are suitable basic states for supporting modes that yield reasonably accurate amplitude modulation. Thus, they both represent typical models that suit our general purposes described at the end of § 1, but there are noticeable defects in case (2) that we were unable to remove. We are therefore going to present the details only for case (1), for which we have also completed the three-step process described in § 2, that is, we went beyond the disk model to construct the model for the spherical component (see § 4). The final model is summarized in § 5. In § 6 we present the theoretical results obtained for this case, through extensive calculations, for comparison with observational data.

At this point, we should mention that the pattern speed $\Omega_p = 24$ km s^{-1} kpc^{-1} for case 1 is within 10% of the value of 26 km s^{-1} kpc^{-1} obtained by Elmegreen et al (1989). There is a simple dynamical reason for this agreement since the other is obtained from the consideration of resonances. This is indeed a happy agreement in the determination of the correct value from two different methods.

4. COMPARISON WITH OBSERVATIONAL DATA

We now describe the comparison with observational data as we follow the steps leading to these computed results. We begin with the discussion of optical features and continue into that of the distribution and motion of the interstellar medium. The analysis of observed density distribution made by Elmegreen et al (1989) is shown in Figure 1. The density distribution was Fourier analyzed, and only the two-armed component is shown here. The messy situation in the central regions may be attributed to the projection of the nuclear bulge. Note the density minimum along the spiral arm at $r \simeq 6$ kpc between two peaks of density distribution. Note also the existence of small scale features which overlay the two-armed large-scale structure.

If we superpose Figure 1 on the spiral mode calculated (Fig. 2*a*), we note good agreement of the large-scale structures, particularly the minimum of density at $r = 6$ kpc. As discussed above, this is an interference minimum typical of a mode maintained by waves propagating in opposite directions as distinct from a single propagating wave.

We also show the comparison of the theoretical and observational data in the plot of the wave amplitude against the radial distance (Fig. 3). Again, we see that the observed features are modified with small-scale irregular features. The corotation radius of the spiral mode lies at $r \simeq 9$ kpc. Thus we are

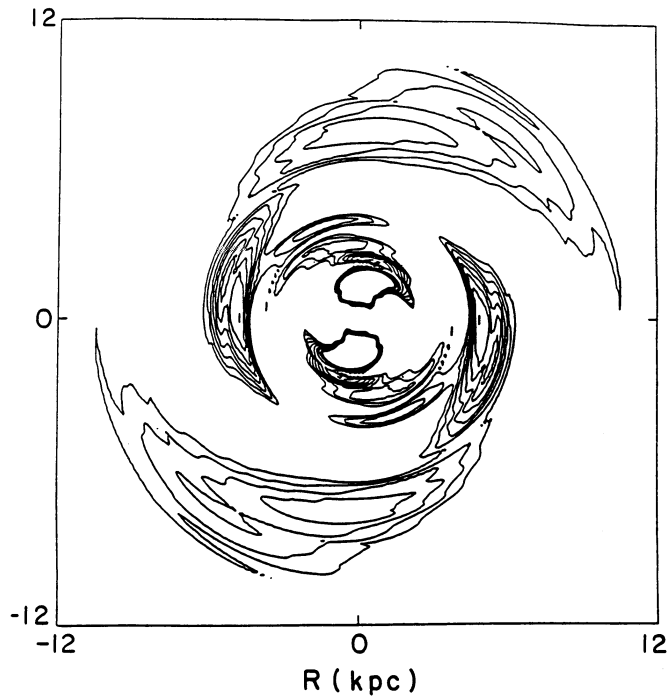

FIG. 1.—Density distribution observed in M81: the two-armed Fourier component ($m = 2$) of the data given by Elmegreen et al. (1989).

showing the outer part of the optical disk as well, where the agreement between simple theory and observation cannot be expected.

The density distribution of the interstellar medium is shown in Figure 4. We note that there are global spiral structures shown even with this cloudy model for the ISM (Roberts 1992). The concentrations are expected to lie near the spiral potential minima, as indeed shown in Figure 5. (In order to get features comparable to the observational data as shown in Fig. 6.18b, p. 125 of Visser [1977], one should perhaps use a slightly different model, possibly with lower velocity dispersion and higher surface density in the outer disk.)

An accurate calculation of the flow field in this cloudy model is not easy, because there may be too few particles to guarantee good averages for each cell of the grid. However, such a calculation has been made which shows reasonable agreement with the data provided in Visser's work (Fig. 6). We should note the wiggles of line-of-sight velocity typical of galactic shocks along spiral arms on both sides of the major axes.

In the calculation of the distribution of the gas and its flow field, the variation of wave amplitude along the spiral arm is important. Note that Visser did not adopt the theoretical amplitude distribution appropriate to a single propagating wave packet, but adopted a distribution in linear segments on the basis of Schweizer's observational data. Yet we both obtained reasonable agreement with observational data. (Visser's diagram shows great regularity because it shows the *theoretical* picture for a *simple* model for the ISM that has no cloudy structure and no self-gravitation. The observational data, which are much more irregular, are obscured in his presentation.)

Finally, we show the characteristics of the basic model obtained in Figure 7. Note that we have a surface density lower (by a factor of 0.6) than that in Visser's model but in agreement with Kent's model. This brings the light-to-mass ratio down to about 4.0 which is in approximate agreement with Kent and closer to what optical observers believe to be typical of Sb galaxies. Dynamically, if the mass density is that suggested by Visser, an open mode leading to a bar-like structure would be likely to prevail (see Paper I). The corotation circle in our

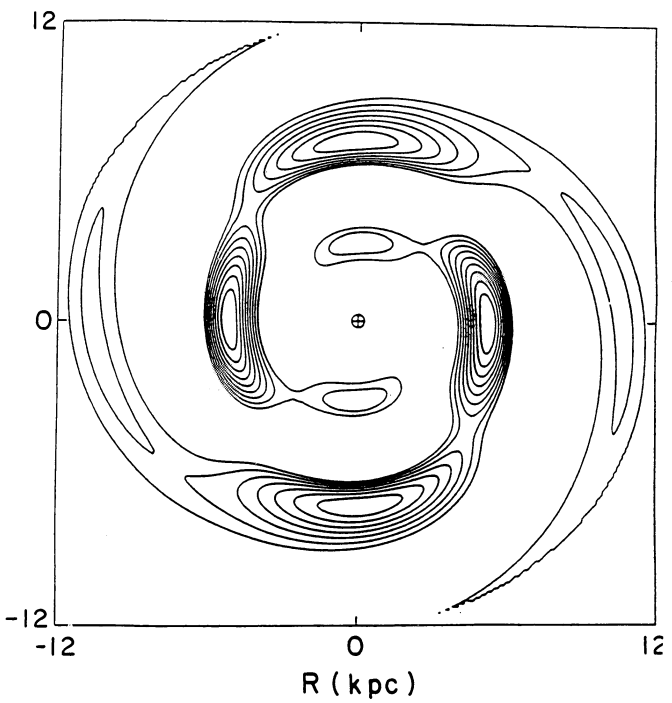

FIG. 2a

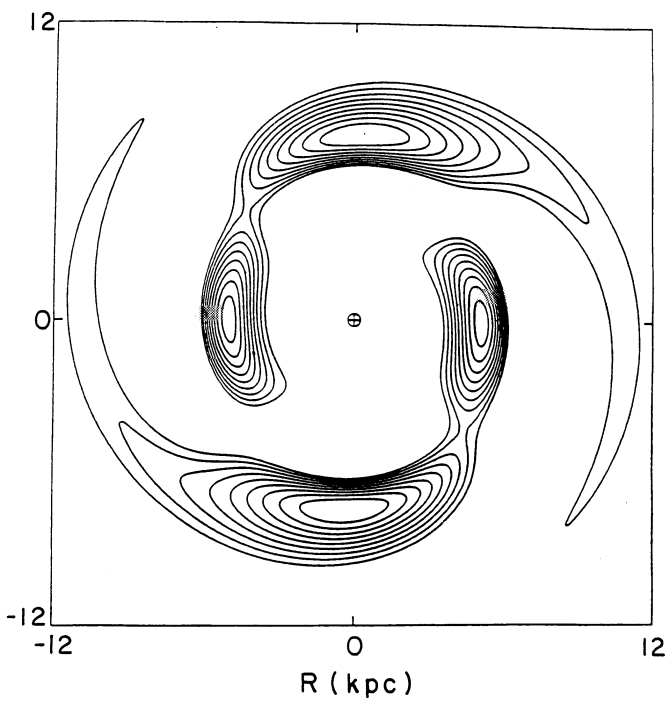

FIG. 2b

FIG. 2.—Amplitude distribution of density waves in the modal pattern computed on the basis of the dynamical model shown in Table 2: (*a*) density, (*b*) potential. Note its generally good agreement with the pattern shown in Fig. 1.

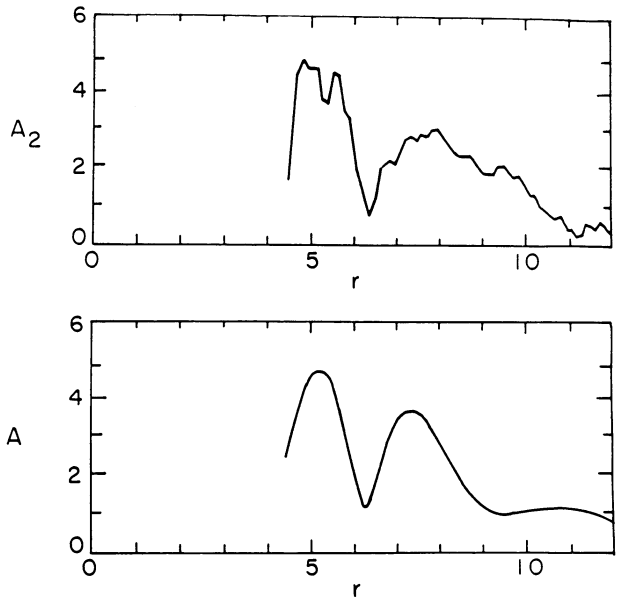

FIG. 3.—Comparison of amplitude distribution along a radial direction from observational data (*upper panel*) and from theoretical prediction (*lower panel*). Note the location of the dip in amplitude slightly within $r = 5$ kpc.

model lies at about 9 kpc which is farther inwards than assumed by Visser, at about 12 kpc.

The spiral structure terminates on the inside at approximately $r = 4$ kpc. There are reports (Michelle Kaufmann 1993, private communication) that there is observed a ring of ultraviolet observation at 2000 Å. Such a ring in Population I objects reminds us of the studies of the 3 kpc arm in our own Galaxy (Yuan & Cheng 1991). The latter is a resonance phenomenon associated with a rapidly rotating short bar at the galactic center. However, this feature is not clearly observable in the overall survey of M81 in ultraviolet (Hill et al. 1992). We shall therefore not speculate on its nature further. Suffice it to say here that a ring structure does not necessarily imply that it is the location of the ILR.

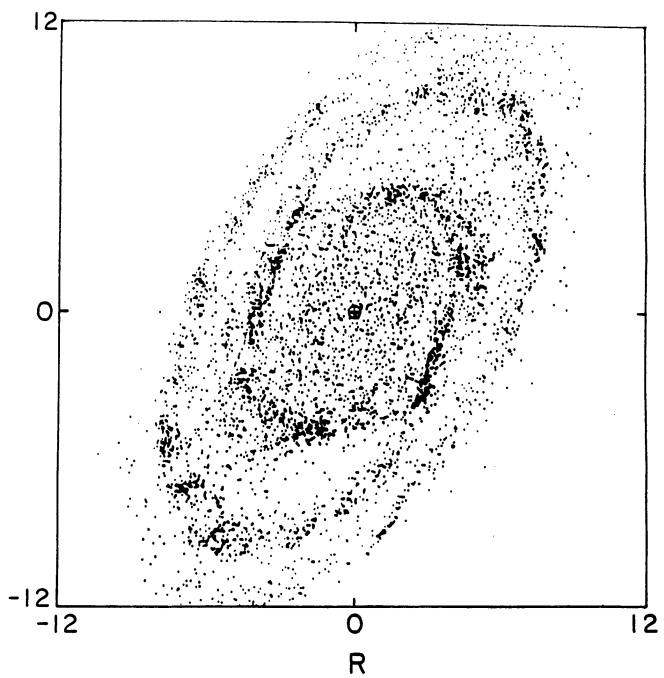

FIG. 4.—Theoretically calculated density distribution of the interstellar medium obtained by using the cloudy model developed by Roberts et al. (1992). Note the limited extent of the development of the spurs and branches of the limited amount of the gaseous component appropriate to M81.

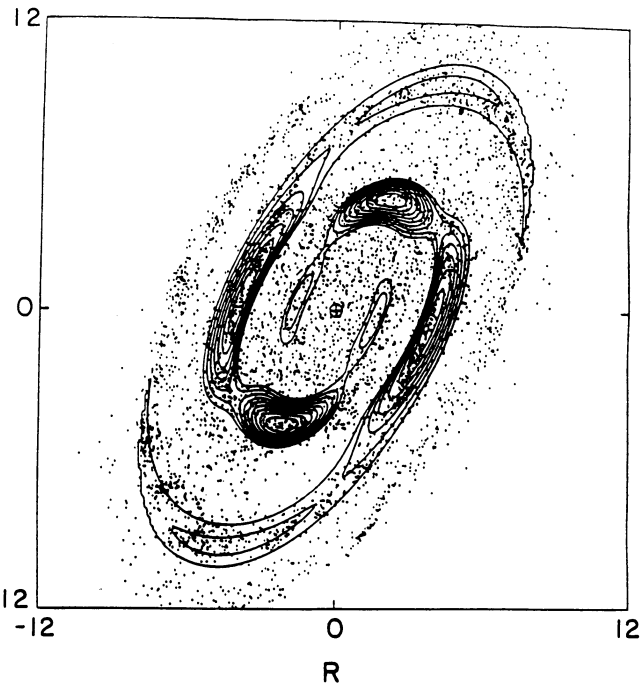

FIG. 5.—Distribution of the interstellar medium compared with the gravitational potential in the theoretical model. Note the concentration of the interstellar medium around the minimum of the gravitational potential.

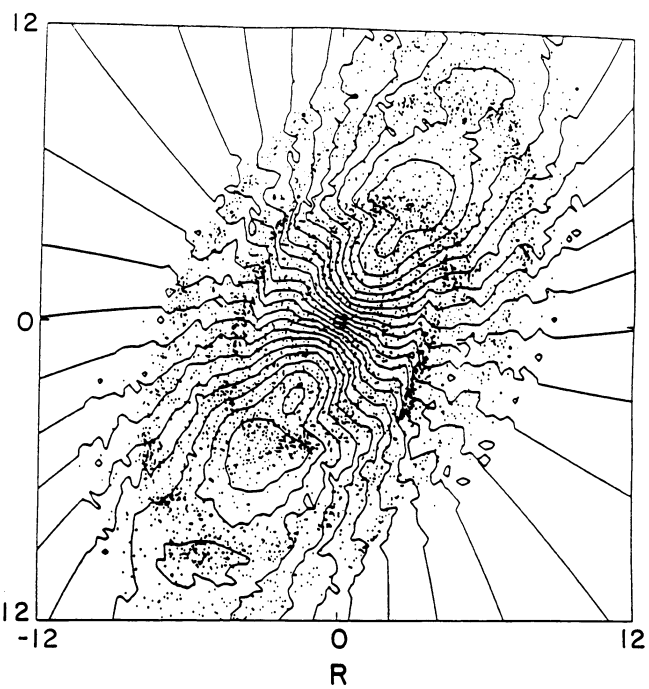

FIG. 6.—Contour map of constant line-of-sight velocity superposed with the distribution of interstellar medium.

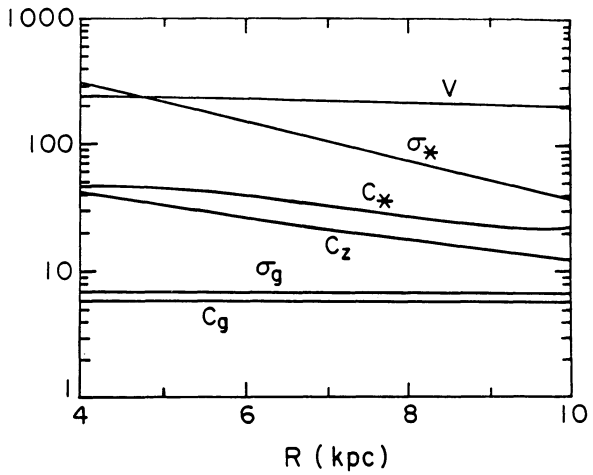

FIG. 7.—Plot of the various parameters in the model of the basic state of the stellar and the gaseous disks.

5. THE MASS MODEL FOR M81

We now turn to the second objective of this paper: the determination of the overall mass model of the galaxy M81, that would support the observed rotation curve and the spiral mode. The density distribution will be specified for all the following three components: (1) the disk components, (2) the nuclear bulge, and (3) the dark halo. As is customary, we assume that there is not a separate dark disk, and we assume that the dark halo has a spherical shape.

The construction of the mass model begins with the rotation curve that is approximated by the formula (3.1a). Its comparison with observational data will be discussed below.

Mass models with bulge components have been extensively studied by Kent (1987a, b) for a number of galaxies. These studies are based on the data for the rotation curve and the luminosity observed for the nuclear bulge and the disk. The same value is usually assumed for the mass-to-luminosity ratio M/L for the bulge and the inner disk. In the case of the galaxy M81, Kent found the value of

$$\frac{M}{L} = 3.76 \frac{M_\odot}{L_\odot},$$

which is considerably different from that used in the model adapted by Visser. (Kent also examined the use of the maximal disk hypothesis, but obtained a model with a [small] negative mass for the nuclear bulge. That model was therefore rejected as being unsatisfactory.)

In the previous section, we have obtained a model for the disk by an entirely different method, that is, without considering the overall distribution of mass. Its mass distribution could therefore be quite different from Kent's model; however, it turned out that they are nearly the same. Our value for $M/L = 4.0\, M_\odot/L_\odot$. Our model has an exponential length scale 2.83 kpc instead of his value of 2.5. The bulge and halo mass distributions are also somewhat different, but the theoretical rotation curves obtained are essentially the same: even the contribution to the rotation curve from the various components are approximately the same. We have, of course, the additional determination of the velocity dispersion of both the radial and the vertical components of stellar velocity dispersion.

The agreement with Kent gives additional evidence that we have found a *mass model*, together with the velocity dispersion in the stellar component, that supports a mode that is a close approximation to the observed spiral structure.

The details of our mass model and its comparison with Kent's model will now be given.

5.1. *The Stellar Disk*

The surface density in the stellar disk is given by

$$\sigma_D = \sigma_0 e^{-r/h_*},$$

as found above, where $\sigma_0 = 1206\, M_\odot\,(\mathrm{pc})^{-2}$ and the exponential length scale $h_* = 2.83$ kpc. For the calculation of the rotation curve, the contribution of the gaseous component may be neglected. (The exponential disk has a mild singularity in the rotation curve near the center, but this is known to be unimportant.)

5.2. *The Nuclear Bulge*

The formula for the volume density is given by (as in Kent's paper)

$$\rho_B = \frac{M_B}{4\pi r_M^3} \frac{1}{x^2(1+x)^2},$$

where $x = r/r_M$. This is known to be a convenient alternative form for the formula given by de Vaucouleurs. The bulge mass $M_B \times 10^{10}\, M_\odot$, and the scale $r_M = 1.5$ kpc was adopted. These values were obtained by fitting the luminosity distribution with observational data. The value of M/L used is that determined from the above studies of dark matter.

5.3. *The Halo Component*

With the mass distributions given for the nuclear bulge and the disk, the mass distribution in the halo component may be determined from the matching of theoretical and observed rotation curves. However, for practical purposes, it is convenient to *adopt* reasonable formulas for the halo mass distribution, and to determine the parameters in the formula adopted from observational data for the rotation curve. We made this calculation for two different formulas:

$$(\alpha)\ \rho_{H_0} = \frac{\rho_{H_0}}{1+x^2}, \quad x = \frac{r}{L_H},$$

$$(\beta)\ \rho_H = \frac{\rho_{H_0}}{(1+x^2)^2}, \quad x = \frac{r}{r_H},$$

where L_{H_0} and r_H are scale parameters of length, and ρ_{H_0} is the scale parameter for mass.

For the first formula, the rotation velocity approaches a constant $(r\pi G\rho_{H_0})^{1/2} L_H$ at large distances (with total mass becoming infinite); for the second formula, the total mass approaches a constant value $M_H = D\pi^2 \rho_{H_0} r_H^3$ (with rotation velocity approaching zero).

Comparison with observational data shows that we should adopt the following values:

1. $L_H = 3$ kpc, $M_H(r = 12) = 3 \times 10^{10}\, M_\odot$,
2. $L_H = 5$ kpc, $M_H = 5 \times 10^{10}\, M_\odot$.

In either case, the theoretical rotation curve agrees with the observational data very well within 15 kpc.

Further details are given in the legend attached to the figures.

6. SUMMARY OF THE MODEL OF THE GALAXY M81 (NGC 3031)

The method of analysis described above is, in principle, an inductive procedure of successive approximations. We start with certain observational data including the spiral structure. We consider certain categories of mass models, including velocity dispersion in the stars and in the gas, based on observational data. We attempt to determine the parameters in the mass model so as to obtain optimal agreement with the data available. This makes it necessary for us to adopt a procedure combining trial and error and successive approximations. We now present a summary of the results obtained. The reader may wish to proceed to the next approximation, if he wishes. There is always room for further refinement.

6.1. *The Mass Model and the Components of Velocity Dispersion*

The overall mass distribution (with an exponential disk with length scale $h_* = 2.83$ kpc), and the rotation curve supported is given in Table 3 (see also Figs. 8, 9, and 10). There are two models, (α) and (β), with different assumptions adopted for the halo mass; both are compatible with the rotation curve observed at large distances (see § 4).

In Table 4 we give further detailed characteristics of the galactic disk including the following items:

(α) the physical model or the (2C/3D) model: a two-component system of stars and gas with a stellar disk of finite thickness;

(β) the dynamical model or the (1C/2D) model: a single fluid system with a disk of zero thickness. (The ratio σ/σ_* is approximately the thickness reduction factor.)

In item (β), the effective mass density is reduced from the actual column density according to the discussions in § 2.

6.2. *Supplementary Information*

The mode calculated and shown in Figure 3 has the following characteristics: (1) Pattern speed $\Omega_p = 24$ km s^{-1} kpc^{-1}, (2) Corotation circle located at $r_{co} = 9$ kpc, (3) Inner turning point $r_{co} \doteq 4$ kpc.

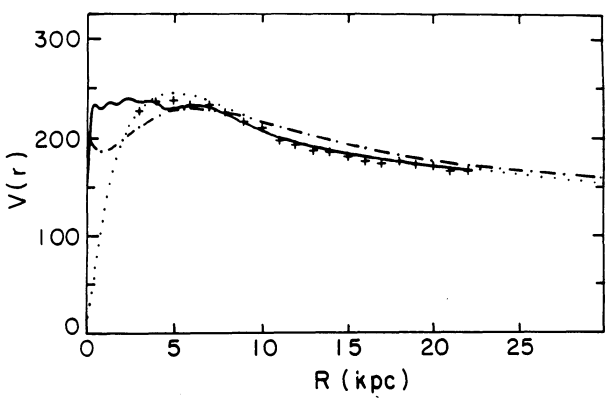

FIG. 8.—Rotation curve of the models compared with observational data. Note that all the theoretical curves compared agree very well with observational data in the range 4 kpc $< r <$ 15 kpc which is significant for the study of spiral structure. *Dotted curve:* rotation curve used in this paper; *solid curve:* rotation curve used by Kent to fit observational data; *dash-dotted curve:* present mass model described in § 5.

TABLE 3

MASS WITHIN A SPHERE OF RADIUS R IN TWO MASS MODELS (IN 10^{10} $M_\odot$)

R	M_D	M_B	M_H	M_T
(α) Case of halo with finite mass				
0.0	0.00	0.00	0.00	0.00
1.0	0.30	0.60	0.01	0.91
2.0	0.96	0.86	0.09	1.91
3.0	1.74	1.00	0.24	2.98
4.0	2.51	1.09	0.46	4.05
5.0	3.20	1.15	0.71	5.07
6.0	3.80	1.20	1.00	6.00
7.0	4.29	1.24	1.31	6.84
8.0	4.69	1.26	1.63	7.59
9.0	5.01	1.29	1.96	8.26
10.0	5.27	1.30	2.30	8.87
11.0	5.46	1.32	2.65	9.43
12.0	5.61	1.33	3.00	9.94
13.0	5.73	1.34	3.35	10.42
14.0	5.81	1.35	3.71	10.88
15.0	5.88	1.36	4.07	11.31
16.0	5.93	1.37	4.43	11.73
17.0	5.96	1.38	4.79	12.13
18.0	5.99	1.38	5.15	12.53
19.0	6.01	1.39	5.52	12.92
20.0	6.03	1.40	5.88	13.31
(β) Case of halo with finite mass				
0.0	0.00	0.00	0.00	0.00
1.0	0.30	0.60	0.02	0.92
2.0	0.96	0.86	0.11	1.93
3.0	1.74	1.00	0.32	3.04
4.0	2.51	1.09	0.60	4.19
5.0	3.20	1.15	0.91	5.26
6.0	3.80	1.20	1.22	6.22
7.0	4.29	1.24	1.52	7.05
8.0	4.69	1.26	1.79	7.75
9.0	5.01	1.29	2.03	8.33
10.0	5.27	1.30	2.25	8.82
11.0	5.46	1.32	2.44	9.22
12.0	5.61	1.33	2.61	9.56
13.0	5.73	1.34	2.76	9.83
14.0	5.81	1.35	2.90	10.07
15.0	5.88	1.36	3.02	10.26
16.0	5.93	1.37	3.13	10.43
17.0	5.96	1.38	3.23	10.57
18.0	5.99	1.38	3.32	10.69
19.0	6.01	1.39	3.40	10.80
20.0	6.03	1.40	3.47	10.89

NOTES.—The symbols M_B, M_D, M_H, and M_T represent, respectively, the mass within radius R of the bulge, disk, halo components, and thin total.

The total luminous mass (bulge and disk) is about 7.43×10^{10} $M_\odot$; this leads to a mass-to-luminosity ratio $M/L = 3.85$, if one adopts the value of total luminosity given by Kent (1987a, b).

The following is supplementary information for the physical model of NGC 3031:

1. Thickness of stellar disk: $z_* = 0.30$ kpc; (c_{*r}, c_{*z}), or some obvious simplified forms of them are, respectively, the velocity dispersion in the radial and in the vertical; σ_* is the surface mass density.

2. Gaseous disk: The surface density σ_g is of the order (5–10) $M_\odot$ (pc)$^{-2}$ (the cases 6 ad 9 have been adopted in the actual calculations); the velocity dispersion is $c_g = 6$ km s^{-1}, and the thickness of the disk is neglected.

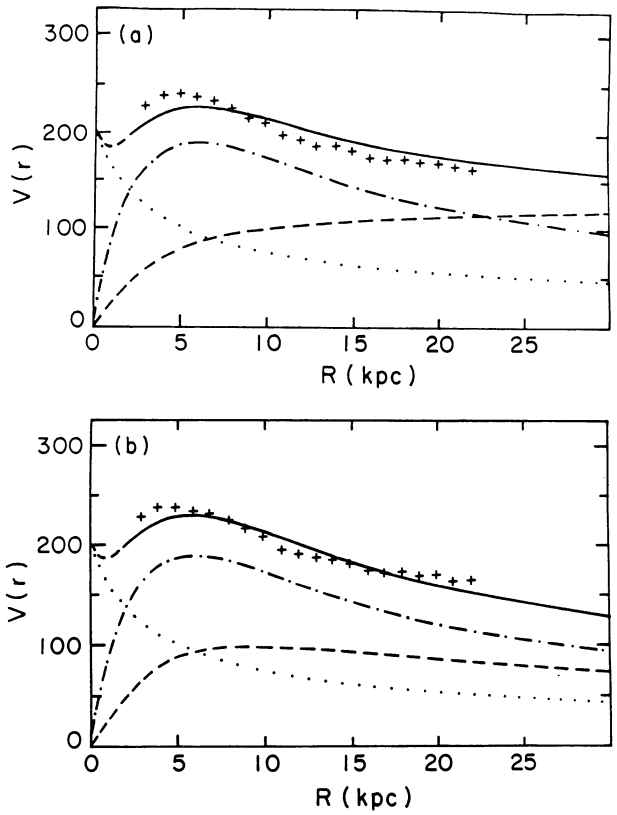

FIG. 9.—Contribution to the rotation curve from individual components: bulge, disk, and halo shown, respectively, as dotted, dashed, and dot-dashed curves. To get the rotation curve for the whole model, one should add the gravitational field of the individual components. The upper diagram refers to case (*a*) with infinite halo mass; the lower diagram refers to case (*b*) with finite halo mass. The difference between the two cases is negligible.

3. The parentheses in Table 5 indicates that the numerical values are no longer reliable or meaningful because the approximation of a thin galactic disk is not expected to be valid as the nuclear bulge is approached. Three-dimensional distribution is clearly indicated when c_{*r} and c_{*z} are nearly equal. For this reason, in Figure 1, the data are shown only for the range 4 kpc $\leq r \leq$ 10 kpc.

6.3. *Supplementary Remarks*

We have essentially demonstrated that, with the self-consistent mass model determined, the observed spiral structure can be supported primarily as a linear mode. As mentioned in § 1, the physical structure is *not* a growing linear mode but a slowly evolving spiral structure with an amplitude limited by nonlinear mechanisms.

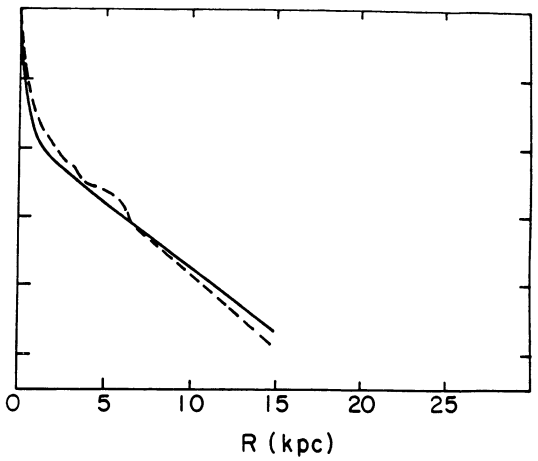

FIG. 10.—Luminosity profile calculated for the present model with $h_* = 2.83$ kpc and $M/L = 4.0\ M_\odot/L_\odot$, shown as a solid line. Comparison is made with that given by Kent with $h_* = 2.5$ kpc and $M/L = 3.76\ M_\odot/L_\odot$.

7. DISCUSSION

As stated earlier, our first principal objective in this paper is to construct a physical model for M81 that is compatible with a number of observational data, including the observed motions of the interstellar medium. Specifically, we impose the requirement that the basic state will support a wave mode that conforms to the observed spiral structure, including the amplitude distribution, which shows a modulation along the spiral arms. Our second objective is to develop a method of analysis that includes the thickness of the stellar component, which has been shown (see Figs. 6 and 10 in Paper I) to be very important for maintaining the proper mode. This method will become increasingly more useful since infrared data are becoming more widely available.

7.1. *The General Nature of the Basic State*

The basic model found is significantly different from that used by Visser in his well-known analysis of the behavior of the interstellar medium in M81. Since his model does not include significant spherical components, his disk mass is much higher, and consequently the spiral structure observed leads him to

TABLE 4

MODEL OF THE DISK OF THE GALAXY NGC 3031

DISTANCE FROM GALACTIC CENTER	CIRCULAR VELOCITY	PHYSICAL MODEL (STARS)			DYNAMICAL MODEL (FLUID	
r (kpc)	V (km s^{-1})	σ^* ($M_\odot$/pc^2)	c^*r (km s^{-1})	c^*z (km s^{-1})	$[\sigma]$ ($M_\odot$/pc^2)	$c_r = c_z$ (km s^{-1})
2	194	595	(45.1)	(49.2)	(154)	(39.4)
3	227	418	(57.1)	(41.2)	(154)	(39.4)
4	240	393	55.6	34.5	151	43.6
5	243	206	49.3	28.9	126	36.8
6	240	145	41.9	24.2	100	31.6
7	235	102	34.8	20.3	77	28.0
8	328	71.4	28.6	17.0	59.4	25.3
9	222	50.1	24.1	14.3	45.9	22.8
10	216	35.2	23.0	12.0	35.8	20.6

TABLE 5

DYNAMICAL AND PHYSICAL MODELS

A. DYNAMICAL MODEL T (FLUID)

r	v	V	κ	σ	Q	J	ϵ_0	c_r	k	f_T
2.....	−0.871	194	168	154	3.16	0.122	0.0371	39.4	4.70	0.244
3.....	−0.855	227	121	172	2.47	0.227	0.0533	47.7	3.14	0.390
4.....	−0.803	240	90	154	1.87	0.326	0.0648	43.6	2.35	0.494
5.....	−0.720	243	68	226	1.47	0.420	0.0734	36.8	1.88	0.569
6.....	−0.601	240	53.4	100	1.25	0.500	0.0790	31.6	1.57	0.625
7.....	−0.445	235	42.9	77	1.15	0.550	0.0810	28.0	1.34	0.668
8.....	−0.257	228	35.5	59.4	1.12	0.568	0.0797	25.3	1.18	0.703
9.....	−0.045	222	30.1	45.9	1.10	0.561	0.0763	22.8	1.05	0.731
10.....	0.186	216	26.0	35.8	1.10	0.541	0.0719	20.6	0.94	0.754

B. PHYSICAL MODEL[a]

r	v	σ_*	c_*	c_z	c_z/c_*	$F_\nu(x)$
2.....	−0.871	595	(45.1)	(49.2)	0.310	(1.090)
3.....	−0.835	418	(57.1)	(41.2)	0.232	(0.722)
4.....	−0.803	292	55.6	34.5	0.250	0.621
5.....	−0.720	206	49.3	28.9	0.301	0.586
6.....	−0.601	145	41.9	24.2	0.376	0.578
7.....	−0.445	102	34.8	20.3	0.468	0.584
8.....	−0.257	71.4	28.6	17.0	0.661	0.596
9.....	−0.045	50.1	24.1	14.3	0.628	0.593
10.....	0.186	35.2	23.0	12.0	0.629	0.520

NOTE.—The parameter Q is not listed, since it does not appear naturally in Shu's dispersion relation. Instead, the parameter $(kc_*/\kappa)^2$ is essential; this parameter is indirectly listed through the response reduction factor $F_\nu(x)$ (see Lin & Shu 1966). The parentheses indicates that the thin disk approximation is no longer valid as the bulge is approached.

[a] Numerical data based on the dispersion relationship (Shu 1968, 1971) for stellar disk of finite thickness and the gaseous disk of zero thickness.

adopt a much smaller pattern speed of 18 km s^{-1} kpc^{-1}. Our resultant mass model, including both the disk and the spherical components, is similar to that found by Kent from his detailed studies of the rotation curve and the nuclear bulge. The global pattern in our model is found to be rotating at an angular speed of about 24 km s^{-1} kpc^{-1}, very close to the value determined by Elmegreen et al. (1989) and to the value determined by Westpfahl (1993) from VLA data of H I velocities, if a single rigidly rotating pattern is assumed.

Apart from the differences in methodology used by various authors (e.g., analytical versus N-particle simulation), a major cause for disagreement in studies of spiral structure is the issue of the *appropriateness of the axially symmetrical basic state of equilibrium adopted* as the initial condition. The differences between the choices made by Aoki et al. (1979), Toomre (1981), and Bertin et al. (1989a, b; Paper I) have been discussed in § II of Paper I (p. 86) and in greater detail by Lin & Lowe (1990). The last deals with models with *inner* wave barriers; both of the other authors deal with models with *outer* wave barriers or no wave barriers. Different basic states would naturally have different modal characteristics.

One important point in appropriate modeling of the basic state is the proper emphasis of the gaseous component; its effect in the *outer disk* is highly significant. Another point is the inclusion of the finite thickness of the stellar disk, which can be highly significant, as shown in Paper I. Indeed, as discussed in § 2.2, finite disk thickness would significantly reduce the impact of the nonlinear effect of the gaseous component on the stellar component. The most important point is the presence or absence of an *inner wave barrier* mentioned above; that is, whether the central region of the galaxy is hospitable to wave propagation. This is usually described in terms of the rising of the parameter Q_* as the center is approached. Different galaxies may have different characteristics in this respect. We assume that M81 does have an inner wave barrier. For such basic states, it is easy to visualize a mode with feedback cycle (see Papers I and II).

7.2. *Alternative Models*

The mode was constructed under certain generally adopted assumptions: one of the most important is that the mass-to-luminosity ratio (M/L) is essentially uniform. (It turns out to be about 4 $M_\odot/L_\odot$.) If this assumption is left open, alternative models are possible. Indeed, another method of modeling two-component disks of finite thickness was given by Bertin (1991) in which the dynamical characteristics of the waves at each location was emphasized. By applying this method, one would get a somewhat different physical model. With the same disk thickness of 0.30 kpc, this new model is found to have an exponential distribution of the surface density with a scale length of 3.5 kpc, somewhat larger than the observed optical length scale of 2.83 kpc. Thus, the mass-to-light ratio M/L would not be exactly constant, but slowly increasing with an exponential length scale of about 16 kpc. This is not unreasonable since there may indeed be a larger fraction of darker stars in the outer disk. This is a good point for further studies.

Since instability characteristics are emphasized in this alternative approach, the compatibility of the two approaches in the neighborhood of the corotation circle should be checked; specifically, the stability parameter should be in approximate agreement. A detailed numerical calculation shows that this is indeed the case (see numerical data in Appendix A). Thus our

general goal is successfully achieved that the modal approach requires only plausible physical basic states to support the observed spiral mode in M81.

We now return briefly to the role of NGC 3077. In contrast to discussions in § 1 of a stable galactic disk being excited by the close passing of the galaxy NGC 3077, Thomasson & Donner (1993) considered a basic state of M81 that appears to be unstable with respect to axisymmetrical perturbations and highly unstable with respect to bisymmetrical disturbances (see § 2, p. 154 of his paper), but they stabilized the system by modifying the nature of the forces of interaction. This is a totally different approach. Indeed, they did not specify the basic state in the manner of our §§ 5 and 6. It is not clear whether they have eventually reached a basic state with very different characteristics. We shall therefore refrain from comparing our analyses with their studies. In the context of our paper, the passage of NGC 3077 might have resulted in a pattern that is a minor perturbation from our mode. The encounter has possibly also changed the orientation of the spiral pattern and influenced the overall amplitudes (see § 1).

The actual history of the formation of the present spiral pattern is naturally very likely related to the passage of NGC 3077. But the present pattern may still be dominated by a single mode as assumed in this paper. The reason is the shortness of the feedback cycle for the formation of the mode and the relatively long time elapsed since the close encounter of the galaxies. There would thus be sufficient time for the nonlinear and dissipative effects to take hold to allow the selective prominance of a single mode.

To demonstrate the relative shortness of the feedback cycle, one may use the discussions of the process of overreflection and numerical calculations of the growth rate (see p. 99ff in Paper II). We found that for galaxy models of the general type considered in this paper, the feedback cycle is generally on the order of one period of revolution of the wave pattern, but usually considerably shorter. According to Thomasson & Donner (see their Fig. 3), the scenario of evolution shows that the closest encounter probably occurred around sometime less than two revolutions ago. (Note however, the difficulty of highly accurate simulation reported by Hernquist 1990 in the case of M51. See also Rix & Ricke 1993.) Thus, the wave pattern has more than two feedback cycles to develop into a mode by the "present time." Since the observational data are restricted to the present instant, it is difficult to ascertain the scenario of past evolution accurately on the basis of such data. We can say, with more certainty, that the observational data are compatible with those expected from a mode over a reasonable basic state for which additional observational check can be made.

7.3. *A Look into the Future*

As shown in § 4, the accurate analysis of data in M81 is somewhat handicapped by the absence of data of good quality in red and in infrared. We adopted the point of view that, in a galaxy like M81, the gas content is not so rich as to cause significant differences between the red and blue spirals, in contrast to that noted by Zwicky in the case of M51. Looking toward the future, as we attempt to apply the methods developed here to other galaxies, we need more precise observational data of the density distribution.

For the gas-rich galaxy NGC 309 (type ScI), Block & Wainscoat (1991) found that the morphology of the underlying density wave of older stars, detected at 2.1 μm, is considerably different from that of the optical image. The multi-armed appearance in blue is replaced by a much more regular two-armed appearance in infrared. This is in line with the pioneering work of Zwicky on the coexistence of spiral morphologies (see also Lin 1971) and is expected (see, e.g., Strom & Strom 1978) within the framework of the density wave theory.

The results of these new observational data are bound to produce important changes in our perception in the density wave theory. The coexistence of different morphologies will naturally lead us to emphasize the distribution of *gravitational potential* which is dominated by the older stars and is free from ambiguity in its structure. Naturally, there is still expected to be coexistence of the slowly varying modal components and the transient nonmodal components. But figures like those shown by Block & Wainscoat can already lead us to important inferences on their roles. The gravitational potential of the impressive nonmodal three-arm component in Population I objects does not produce a correspondingly significant modification in two-armed structure of the primary density distribution. There is thus no clear indication that the dynamics of the global structure is locally modified by the gravitational field of the gaseous component in a serious manner.

The future studies of the density wave theory—in particular the modal approach—has indeed received a substantial boost from these infrared observations. As better and better data become available in more and more galaxies of different types, our understanding of the dynamic mechanisms will also be substantially improved. In the case of NGC 3031, both intrinsic mechanisms and external forcing by NGC 3077 influence its spiral structure. However, if we were to seek a definite answer to the broader question "what fraction of the global grand designs observed in nonbarred spiral galaxies is *primarily* (1) intrinsic in nature, (2) externally driven, or (3) produced by a combination of both mechanisms?" we would find that the ultimate truth is as yet unknown and probably not easy to determine.

We wish to thank Bruce Elmegreen and Frank Shu for their advice and help. Through the help of Elmegreen, acting as the referee, the paper has been considerably improved. C. C. L. wishes to thank C. Hunter for his hospitality during his stay at Florida State University. The work was partly supported by the National Science Foundation.

APPENDIX A

DETAILED STRUCTURE OF THE GALACTIC DISK: SYMBOLS AND DATA

A1. THE DYNAMICAL MODEL (1C/2D MODEL)

In the model studied, the distribution of circular velocity, surface density, and stability parameter are given as follows:

$$V(r) = V_{OD}\left[1 + \left(\frac{r_\Omega}{r}\right)^2\right]^{-1/2}\left[1 + \left(\frac{r}{r_s}\right)^4\right]^{1/4(s_{OD}-1)},$$

$$\sigma(r) = \sigma_0 \exp\left(-\frac{r}{h_*}\right) f\left(\frac{r}{6h_*}\right) + \sigma_g,$$

$$Q(r) = Q_{OD}\left[1 + q \exp\left(-\frac{r^2}{r_Q^2}\right)\right],$$

where

$$f(x) = \begin{cases} 1 - (1 + 4x)(1 - x)^4, & \text{if } x < 1 \\ 1, & \text{if } x > 1. \end{cases}$$

Survey was made to yield a mode that matches the data of Elmegreen et al. (1989). The following parameter values were obtained:

$$V_{OD} = \text{ km s}^{-1}, \quad r_\Omega = \text{ km s}^{-1}, \quad r_s = 5.3 \text{ km s}^{-1}, \quad S_{OD} = 1.34, \quad h_* = 2.83 \text{ kpc}, \quad \sigma_0 = 1206\ M_\odot \text{ pc}^{-2},$$
$$\sigma_g = 6.00\ M_\odot \text{ pc}^{-2}, \quad Q_{OD} = 1.1, \quad q = 2.6, \quad r_Q = 3.5 \text{ kpc}.$$

A2. THE PHYSICAL MODEL (2C/3D MODEL)

Recently we have further altered the basic state density by the introduction of the "T-Model." The density for this model is defined by

$$\sigma_{T_*}(r) = \sigma_0(1 + \Delta)\left[e^{-r/h} f_T\left(\frac{r}{r_{\text{cut}}}\right)\right], \tag{A1}$$

$$\sigma_T(r) = \sigma_{T_*}(r) + \sigma_g \tag{A2}$$

where

$$f_T(x) = \exp\left\{-\frac{1}{6x}\left[1 + w \exp\left(-16x^2\right)\right]\right\}. \tag{A3}$$

Physically, it is simply the formula

$$\sigma_{\text{eff}} = \hat{\sigma}_0 \exp\left(-r/h_*\right) T(k/z_*),$$

where T is the thickness reduction factor of Shu (1971) or Vandervoort (1970). We take $T(x) = e^{-x}$. Calculations of the mode have been made for a suitable selection of parameters to allow the density distribution to match that obtained in the E-model. In the "standard case" of 6/28, we have adopted the following set of parameters:

$$V_{OD} = 275, \quad r_\Omega = 2, \quad r_s = 5.3, \quad s_\infty = 1.34, \quad Q_\infty = 1.10, \quad r_Q = 3.5, \quad q = 2.6, \quad h_m = 2.83,$$
$$r_{\text{cut}} = 17, \quad \sigma_{0m} = 1242, \quad \sigma_{gm} = 9.275, \quad r_0 = 0, \quad z_0 = 0.30, \quad w = 0, \quad m = 2, \quad i = 12, \quad \Omega_p = 24.$$

A3. TABLE FOR THE PHYSICAL MODEL (STELLAR/GAS)

For the physical model, we take a stellar disk of finite thickness, which is assumed to be uniform as a first approximation (on the basis of observational data in a number of other external galaxies). We recognize the existence of nuclear bulge under which only a limited amount of disk mass may be assigned. Since the modal calculation cannot yet be made for a three-dimensional configuration, we are limiting our analysis to the part of a disk with a spiral structure, that is, for $r \geq 4$.

Both the stellar disk and the gaseous disk are prescribed by the set of three parameters (σ, c, z) the mass surface density, the velocity dispersion in the radial direction, and the thickness; the last quantity is related to the vertical velocity dispersion c_z. For our particular model, we adopt $z_* = 0.30$ kpc and $(\sigma_g, c_g, z_g) = (9.275, 6, 0)$ in units of $[M_\odot (\text{pc})^{-2}, \text{km s}^{-1} \text{ kpc}^{-1}]$.

By using Shu's dispersion relationship, with $T(x)$ approximated by e^{-x}, we may calculate $c_*(r)$ if $k(r)$ is given on the basis of the calculated mode in the dynamical model if this mode is in good agreement with the observed density distribution (Elmegreen's Fourier decomposition).

In this model, the amount of gas was set slightly higher than expected to ensure more stability in the stellar component and technical convenience in modal calculation. A model with somewhat less gas and smaller thickness would perhaps be more realistic (e.g., $\sigma_H = 5$, $\sigma_g = 7\ M_\odot\ [\text{pc}]^{-2}$ if primordial helium and other gases are included). But the differences are expected to be small (see discussion below) except possibly for the growth rate; but this parameter is, in any case, controlled during the modal calculation by fine tuning of Q_{eq} in the dynamical model (see Tables 1 and 2). We should also note that we are using a linear theory while the dynamical behavior of gas is likely to be nonlinear in the real galaxy.

With our present framework, the stability parameter for stars alone suggests stability with respect to axisymmetric perturbations, but the effect of gas brings it down to the marginal condition. This has been checked by using the relationship (Lin & Shu 1966; Bertin & Romeo 1988)

$$\bar{Q}_* = 1 + 2\sigma_g/\bar{\sigma}_*$$

for marginal stability with respect to axisymmetric perturbations in a two component system with zero disk thickness. The reduction factor $f_T = T(x)$ has been used to relate our present model to that idealized case:

$$\bar{\sigma}_* = \sigma_* f_T , \qquad \bar{Q}_* = Q_*/f_T .$$

With the numerical values tabulated for κ, c_*, σ_* at $r = 9$ kpc (where $v \doteq 0$) we find that the agreement is within 3%. Thus, the increase of Q_{eq} from unity for any decrease of σ_g is $\Delta Q_{eq} = -\Delta\sigma_g/\bar{\sigma}$ and amounts to a value $\leq 0, 1$ for $\Delta\sigma_g = -2\ M_\odot\ (\mathrm{pc})^{-2}$. With the current progress made in the study of the instability of disks of finite thickness (see Romeo 1992), the accuracy of the approximations adopted should be reexamined; but we do not expect major changes.

APPENDIX B

SOME FURTHER DISCUSSION OF MODEL FOR M81

In § 3 we presented two dynamical equivalent versions of a model for M81: a two-component model of stars and gas and a one-component fluid model for the calculation of the spiral model. One may note that there is a minor but notable systematic difference between the values of velocity dispersion for the two models. This is caused in part by the difference in disk thickness (being finite for the stellar disk, zero for the fluid model) but more importantly the difference in the appropriate dispersion relationship for the two systems. The reconciliation of these differences is indicated in the following calculations and summarized in Table 6.

B1. GENERAL COMMENTS

The model is obtained through the use of the dispersion relationship given by Frank Shu in his lecture at Brandeis University (1971), similar to Visser's work. It differs from the latter mainly in the value adopted for the mass-to-light ratio M/L. The value of 4 $M_\odot/L_\odot$ is obtained in this paper (see discussion by van Albada & Sancisi 1986 of dark matter and models of galaxies). The velocity dispersion is also about half as much as given by Visser.

B2. THE STAR-GAS MODEL, SOME DETAILS

The stellar component has a uniform disk thickness of 0.3 kpc. The mass density is given by an exponential formula

$$\sigma_* = \hat{\sigma} e^{-r/h_*} .$$

We took $M/L = 6\ M_\odot/L_\odot$, so that $\hat{\sigma} = 1206\ M_\odot\ (\mathrm{pc})^{-2}$. Observational data give $h_* = 2.83$ kpc for best fit.

Observational data and modal calculations suggest that $\Omega_p \lesssim 24$ km s^{-1} kpc^{-1}. The following table is based on the value of 24, although similar results can be obtained for lower values of Ω_p. We also take the pitch angle to be 12°; again variations of pitch angle can be easily made. Small changes, for example, 10% in Ω_p and pitch angle yield minor changes in the velocity dispersion obtained.

All the symbols used in Table 6 are essentially the same as in Shu (1971).

The thickness of the stellar disk is taken to be 0.3 kpc, that of the gaseous disk is negligible; $\sigma_g = 9\ M_\odot$, $c_g = 6$ km s^{-1}.

In the above table $[c_r]$ c_r are the values for the corresponding fluid models. The value $[c_r]$ is obtained from c_{r*} by a conversion procedure, by equating the reduction factors for the fluid model and the stellar model:

$$F_\nu^{(g)}(x_g) = F_\nu(x_*) ;$$

thus,

$$x_g = (1 - \nu^2)\{[F_\nu(x_*)]^{-1} - 1\} ,$$

$$x_g = k^2[c_r]^2/k^2 .$$

The value c_r is obtained from modal calculation. The pair of values (σ, c) in the fluid model were adjusted to yield the correct pattern, with $\sigma(r)$ given by

$$\sigma(r) = \sigma_*(r)T_{**} + \sigma_g T_{gg} ,$$

where the symbols are the same as in Shu (1971).

B3. DISCUSSION OF THE GAS CONTENT

The gas content for the above calculations is taken to be $\sigma_g = 9\ M_\odot\ (\mathrm{pc})^{-2}$. Another calculation was made for $\sigma_g = 6$. The results were not greatly different from each other.

We took $\sigma_{\mathrm{H\,I}}$ to be about 5 $M_\odot\ (\mathrm{pc})^{-2}$ (with the advice of Morton Roberts). With the He/H ratio about 0.4, we get $\sigma_g = 7\ M_\odot\ (\mathrm{pc})^{-2}$.

TABLE 6

COMPARISON OF STELLAR AND GASEOUS DISKS

r	σ_*	c_{r*}	c_{z*}/c_{r*}	$[c_r]$	c_r
3.....	418	57	0.72	...	48
5.....	206	49	0.59	38	37
7.....	202	35	0.58	31	28
9.....	50	24	0.59	22	23

B4. MODAL SUPPORT

To confirm that the mode used above is indeed self-consistent, we shall now make two simple checks here. First, the phase integral for the waves for a complete feedback cycle should be an odd multiple of π (Lau, Lin, & Mark 1976). Indeed, this is easily checked to be approximately satisfied. We find that

$$\oint k\,dr = 2\int_{r_{ce}}^{r_{co}} |k|\,dr \cong 5\pi$$

for a pattern with pitch angle of 12° with $r_{ce} = 4$ kpc and $r_{co} = 9$ kpc. Second, the group velocity of propagation for the waves over the physical model for the disk of finite thickness should be approximately the same as that for the dynamical model. This is expected to be approximately true in general from the following argument. As long as the wave number $k(r)$ is matched for two wave patterns with reasonable accuracy, the group velocities of the two patterns would be the same with an accuracy up to the factor $1 + O(c_g/\kappa r)$. To see this, consider

$$r\frac{dk}{dr} = \frac{\partial k}{\partial v}\frac{\partial v}{\partial r} + O(1)$$

where $\partial k/\partial v$ is based on the local dispersion relationship and $O(1)$ represents the effect of the gradient of parameters of the basic state. For example, $r(\partial v/\partial r) = O(1)$. Since

$$r\frac{\partial k}{\partial v} = \frac{\kappa r}{c_g} \gg 1\ ,$$

the above statement is confirmed.

REFERENCES

Aoki, S., Noguchi, M., & Iye, M. 1979, PASJ, 31, 737
Bertin, G. 1990a, in Windows on Galaxies, ed. G. Fabbiano et al. (Dordrecht: Kluwer), 341
———. 1990b, Ann. NY Acad. Sci., 596. 123
———. 1991, in IAU Symp. 146, Dynamics of Galaxies and Molecular Cloud Distribution, ed. F. Combes & F. Casoli (Dordrecht: Kluwer), 93
———. 1993, PASP, 105, 640
Bertin, G., Lau, Y. Y., Lin, C. C., Mark, J. W. K., & Sugiyama, L. 1977. Proc. Nat. Acad. Sci., 74, 4726
Bertin, G., Lin, C. C., Lowe, S. A., & Thurstans, R. P. 1989a, ApJ, 338, 78 (Paper I)
———. 1989b, ApJ, 338, 104 (Paper II)
Bertin, G., & Romeo, A. B. 1988, A&A, 195, 105
Binney, J., & Tremaine, S. 1988, Galactic Dynamics (Princeton: Princeton Univ. Press)
Block, D. L., & Wainscoat, R. J. 1991, Nature, 353, 48
Elmegreen, B. G. 1990, Ann. NY Acad. Sci., 596, 40
———. 1991, in IAU Symp. 146, Dynamics of Galaxies and Molecular Cloud Distribution, ed. F. Combes & F. Casoli (Dordrecht: Kluwer), 113
———. 1992, Ann. NY Acad. Sci., 675, 183
Elmegreen, B. G., Elmegreen, D. M., & Montenegro, L. 1993, PASP, 105, 644
Elmegreen, B. G., Elmegreen, D. M., & Seiden, P. E. 1989, ApJ, 343, 602
Elmegreen, B. G., & Montenegro, L. 1992, ApJS, 79, 37
Elmegreen, B. G., & Thomasson, M. 1993, A&A, 272, 37
Hernquist, L. 1990, in Dynamics and Interactions of Galaxies, ed. R. Wielen (Heidelberg: Springer), 108
Hewitt, J. N. 1991, BAAS, 23, 393 (Item K)
Hill, J. K., et al. 1992, ApJ, 395, L37
Kaufman, M., et al. 1989, ApJ, 223, 539
Kaufman, M., Bash, F. N., Hine, B., Rots, A. H., Elmegreen, D. M., & Hodge, P. W. 1989, ApJ, 345, 674
Kaufman, M., Elmegreen, D. M., & Bash, F. N. 1989, ApJ, 345, 697
Kent, S. M. 1987a, AJ, 93, 816
———. 1987b, AJ, 93, 1062
Lau, Y. Y., Lin, C. C., & Mark, J. W.-K. 1976, Proc. Nat. Acad. Sci., 73, 1379
Lewis, J. R., & Freeman, K. C. 1989, AJ, 97, 139
Lin, C. C. 1971, Theory of Spiral Structure in Highlights of Astronomy, ed. C. De Jager (Dordrecht: Kluwer), Vol. 2, 88
Lin, C. C., & Lau, Y. Y. 1975, SIAM J. Appl. Math., 29, 352
———. 1979, Studies Appl. Math., 140, 646
Lin, C. C., & Lowe, S. A. 1990, Ann. NY Acad. Sci., 596, 80
Lin, C. C., & Shu, F. H. 1966, Proc. Nat. Acad. Sci., 55, 229
Lin, C. C., Yuan, C., & Shu, F. H. 1969, ApJ, 155, 721
Lubow, S. 1988, in Proc. Symp. in Honor of C. C. Lin, ed. D. J. Benney, F. H. Shu, & C. Yuan (Singapore: World Scientific), 310
Lubow, S. H., Balbus, S. A., & Cowie, L. L. 1986, ApJ, 309, 496
Rix, H. W., & Ricki, M. J. 1993, ApJ, 418, 123
Roberts, W. W. 1992, Ann. NY Acad. Sci., 675, 93
———. 1992, PASP, 105, 670
Roberts, W. W., et al. 1992, ApJ, submitted
Romeo, A. B. 1992, MNRAS, 256, 307
Rots, A. H. 1975, A&A, 45, 43
Rots, A. H., Bosma, A., van der Hulst, J. M., Athanassoula, E., & Coraine, P. S. 1990, AJ, 100, 387
Rots, A. H., & Shane, W. W. 1975, A&A, 45, 25
Schweizer, F. 1976, ApJ, 31, 313
Shu, F. H. 1968, Ph.D. thesis, Harvard Univ.
———. 1971, in Astrophysics and General Relativity, vol. 2, ed. M. Chrétian, S. Deser, & J. Goldstein (New York: Gordon & Breach), 314
Strom, S. E., & Stern, K. M. 1978, in IAU Symp. 77, Structure and Properties of Nearby Galaxies, ed. E. M. Berkhuijsen & R. Wieblinski (Dordrecht: Reidel), 69
Thomasson, M., & Donner, K. J. 1993, A&A, 272, 153
Thomasson, M., Elmegreen, B. G., Danner, K. J., & Sundelius, B. 1990, ApJ, 356, L9
Toomre, A. 1981, in The Structure and Evolution of Normal Galaxies, ed. S. M. Fall & D. Lynden Bell (Cambridge: Cambridge Univ. Press), 111
Toomre, A., & Kalnajs, A. J. 1991, in Dynamics of Disk Galaxies, ed. B. Sundelius (Göteborga University), 341
van Albeda, T. S., & Sancisi, R. 1986, Phil. Trans. R. Soc. Lond. A, 320, 447
Vandervoort, P. O. 1970, ApJ, 161, 87
Visser, H. C. D. 1977, Ph.D. thesis, Univ. Groningen
———. 1980, A&A, 88, 149
———. 1980, A&A, 88, 159
Westpfahl, D. J. 1993, ApJ, submitted
Yuan, C. 1987, ApJ, 281, 600
———. 1993, PASP, 105, 657
Yuan, C., & Cheng, Y. 1988, in The Outer Galaxies, ed. L. Blitz & J. Kockman (Berlin: Springer), 144
———. 1989, ApJ, 340, 216
———. 1991, ApJ, 376, 104
Yue, Z. Y. 1982, Geophys. Astrophys. Fluid Dyn., 20, 1